Photoassociation of ultracold RbCs molecules into the (2)0^- state ($v = 189, 190$) below the $5S_{1/2}$ + $6P_{1/2}$ dissociation limit*

Chang Xue-Fang(常雪芳), Ji Zhong-Hua(姬中华), Yuan Jin-Peng(元晋鹏), Zhao Yan-Ting(赵延霆)†, Yang Yong-Gang(杨勇刚), Xiao Lian-Tuan(肖连团), and Jia Suo-Tang(贾锁堂)

State Key Laboratory of Quantum Optics and Quantum Optics Devices, Laser Spectroscopy Laboratory, Shanxi University, Taiyuan 030006, *China*

(Received 4 January 2013; revised manuscript received 12 March 2013)

Ultracold polar RbCs molecules are produced via photoassociation in a laser-cooled mixture of ^{85}Rb and ^{133}Cs atoms. The $a^3\Sigma^+$ state molecules which decay from electronically excited (2)0^- state RbCs molecules are detected by resonance-enhanced two-photon ionization. The new rovibrational levels ($v = 189$, 190) in the (2)0^- state are also observed, which exist in theory and have not been observed in experiments yet. The corresponding rotational constants are measured by photoassociation spectroscopy, which are consistent with theoretical calculations using a nonrigid rotor model.

Keywords: photoassociation technique, ultracold RbCs molecules, rovibrational spectroscopy

PACS: 37.10.–x, 34.80.Gs, 34.50.Ez, 33.20.Vq **DOI:** 10.1088/1674-1056/22/9/093701

1. Introduction

Ultracold polar molecules have been of special interest because of their low temperatures, permanent dipole moments, and long-range anisotropic dipole–dipole interactions, which allow the formation of molecular Bose–Einstein condensate (BEC), manipulation with external electric fields, and preparation of entangled quantum states, respectively. Ultracold polar molecules have been widely used in high-resolution spectroscopy,[1] ultracold collisions,[2] ultracold chemistry,[3] quantum information, and quantum computing.[4]

There are two primary methods used to produce molecules in the sub-milli-kelvin temperature range, which are magnetically tunable Feshbach resonance[5] and light-assisted photoassociation (PA).[6] Although the Feshbach resonance is a highly sufficient method to produce molecules in vibrational levels of the electronic ground state, this method has a high demand on the atomic sample. On the contrary, the photoassociation technique can be realized in all cases of homonuclear[7] and heteronuclear molecules.[8] The PA technique has been used to form many polar species with two different alkali atoms, for example, RbCs,[1] KRb,[9] NaCs,[10] and LiCs.[11] With the help of the PA technique, we can obtain ultracold molecular information of excited states and the ground state, which is useful for characterizing molecular level parameters and investigating the molecular dynamic properties.

We choose RbCs molecules as our research sample for several reasons. As RbCs molecules are bosons, they are suitable candidates for a BEC of polar molecules. The RbCs molecules in the ground state are stable and do not have an atom exchange reaction in the form of RbCs + RbCs $\rightarrow$ Rb_2+ Cs_2 in the rovibrational ground state. RbCs molecules each have a large Frank–Condon factor (FCF)[12] and can serve as a qubit in quantum information processing. Recently, experiments based on RbCs molecules have been conducted and some exciting results have been obtained. A stimulated Raman adiabatic passage (STIRAP) scheme was used to produce RbCs molecules in the rovibrational ground state with high phase-space density.[13,14] The methods of resonance coupling, either $(1)^1\Pi \sim (2)^1\Pi$[15] or $A^1\Sigma^+ \sim b^3\Pi$,[16] were explored for the formation of RbCs molecules in the lowest rovibrational ground state. A detailed investigation has been made for the photoassociative formation of RbCs molecules in the excited $(2)^3\Pi$ state correlated to $v = 8$, (5)0^+ vibrational level.[1] A different formation path of triplet RbCs molecules was reported, which involves the PA near the previously non-investigated region of the Rb($5S_{1/2}$) + Cs($6P_{3/2}$) dissociation limit followed by radiative stabilization. The produced molecules were detected by resonance-enhanced two-photon ionization (RETPI) through the previously unobserved $(3)^3\Pi \leftarrow a^3\Sigma^+$ band.[17] From the PA spectrum of the (2)0^- state, we can have a good knowledge of the structure of the lowest excited state of RbCs. It is meaningful to choose the most suitable path to produce ultracold RbCs in the ground state.

In this paper, we report on the photoassociative production of electronically excited polar RbCs* molecules correlated to Rb($5S_{1/2}$) + Cs($6P_{1/2}$) dissociation and the detection of RbCs molecules in the triplet state. The triplet state

*Project supported by the National Basic Research Program of China (Grant No. 2012CB921603), the International Science & Technology Cooperation Program of China (Grant No. 2011DFA12490), the National Natural Science Foundation of China (Grant Nos. 61275209, 10934004, and 11004125), and the National Natural Science Foundation for Excellent Research Team, China (Grant No. 61121064).

†Corresponding author. E-mail: zhaoyt@sxu.edu.cn

© 2013 Chinese Physical Society and IOP Publishing Ltd

RbCs molecules are observed by the RETPI technique. We observe the rovibrational levels of $(2)0^-$ state ($v = 189$, 190), which exist in theory but have not been observed experimentally before. According to the nonrigid rotor model, we analyze the photoassociation spectrum and obtain corresponding rotational constants, which are consistent with the theoretical calculations.

2. Experimental scheme and setup

Figure 1 shows the formation and ionization scheme of RbCs molecules. Two colliding ultracold ^{85}Rb($5S_{1/2}$, $F = 2$) and ^{133}Cs($6S_{1/2}$, $F = 3$) atoms are photoassociated into a weakly bound, electronically excited $(2)0^-$ state molecular level correlated to the Rb($5S_{1/2}$) + Cs($6P_{1/2}$) dissociation limit. As the excited-state molecular life is short, these molecules will soon decay either to the metastable $a^3\Sigma^+$ ground state or back to free Rb and Cs atoms. Then, molecules in $a^3\Sigma^+$ state are ionized by the RETPI through the $3^3\Pi$ intermediate state correlated to the Rb($5S_{1/2}$) + Cs($5D_{3/2,\ 5/2}$) atomic asymptote.

The experimental setup is shown in Fig. 2. We cool and trap ^{85}Rb and ^{133}Cs atoms in a dual-species, forced dark magneto-optical trap (MOT),[18] which is produced in a stainless-steel chamber with a background pressure of about 4.6×10^{-7} Pa. A pair of coils with anti-Helmholtz configuration generates a magnetic gradient of 12 G/cm, and three other pairs of coils generate a compensate geomagnetism at the position of cold atom clouds. Trapping and repumping beams are provided by four Littrow external-cavity diode lasers (DL100, Toptica), which are locked by the saturated absorption spectroscopy technique. Rb and Cs trapping beams are tuned by acousto-optic modulators (AOMs) to 12.5 MHz and 15 MHz below ($5S_{1/2}$, $F = 3$) $\rightarrow$ ($5P_{3/2}$, $F' = 4$) transition and ($6S_{1/2}$, $F = 4$) $\rightarrow$ ($6P_{3/2}$, $F' = 5$) transition, respectively. The trapping beam powers are 30 mW and 50 mW for Rb and Cs atomic clouds. The Rb and Cs repumping beams are adjusted to ($5S_{1/2}$, $F = 2$) $\rightarrow$ ($5P_{3/2}$, $F' = 3$) and ($6S_{1/2}$, $F = 3$) $\rightarrow$ ($6P_{3/2}$, $F' = 4$) transition, respectively. Each repumping beam has a power of 2 mW. Both trapping and repumping beams are 15 mm in diameter. The depumping beams are separated from the trapping beams by passing through two polarizing beam splitters (PBSs). With the adjustment of other two AOMs, the frequencies are tuned to ($5S_{1/2}$, $F = 3$) $\rightarrow$ ($5P_{3/2}$, $F' = 2$) and ($6S_{1/2}$, $F = 4$) $\rightarrow$ ($6P_{3/2}$, $F' = 4$) transitions, respectively. The depumping beams each

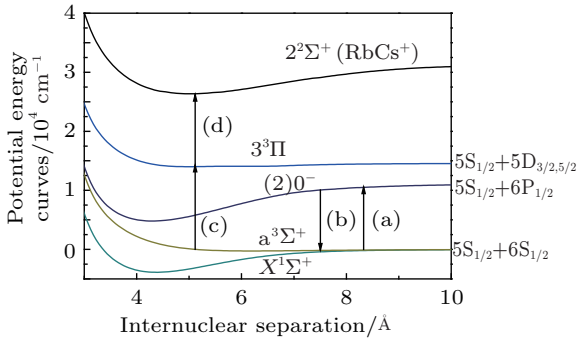


Fig. 1. (color online) (a) Formation and detection scheme of ultracold RbCs molecules produced by a photoassociation laser. Two colliding ultracold ^{85}Rb($5S_{1/2}$, $F = 2$) and ^{133}Cs($6S_{1/2}$, $F = 3$) atoms are photoassociated into a weakly bound, electronically excited $(2)0^-$ state molecular level correlated to the Rb($5S_{1/2}$) + Cs($6P_{1/2}$) dissociation limit. (b) The spontaneous radiation is followed to form a metastable $a^3\Sigma^+$ state molecule. (c, d) The metastable $a^3\Sigma^+$ molecules are ionized by resonance-enhanced two-photon ionization through the $3^3\Pi$ intermediate state correlated to the Rb($5S_{1/2}$) + Cs($5D_{3/2,\ 5/2}$) atomic asymptote.

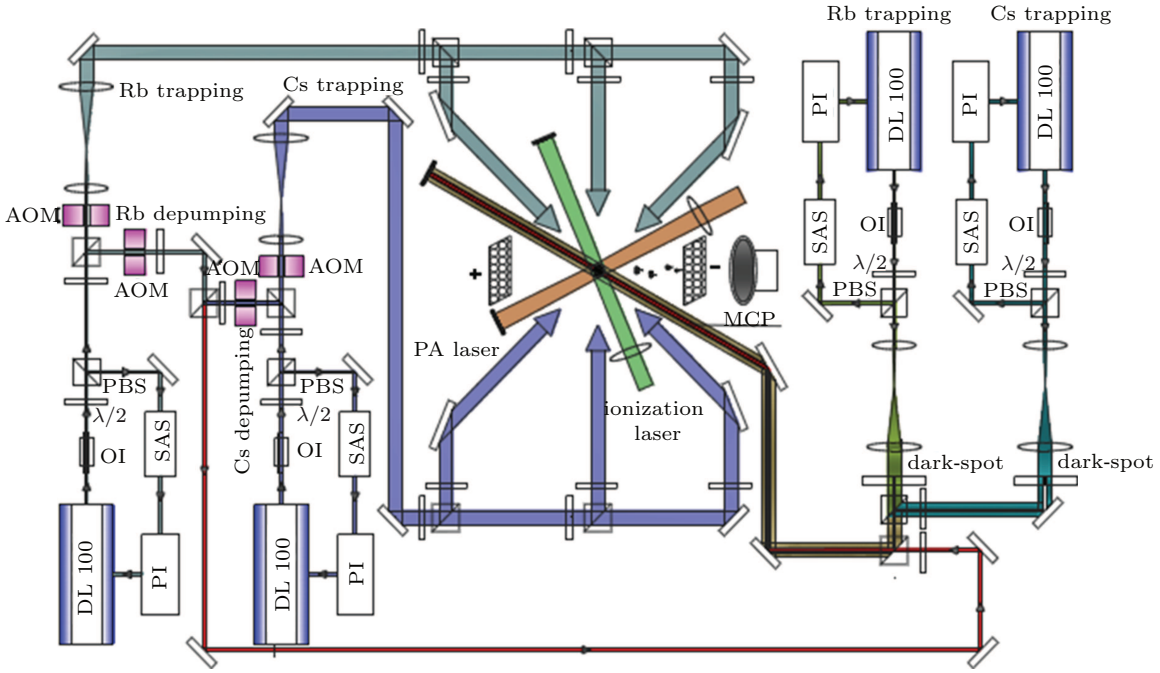


Fig. 2. (color online) Experimental setup. SAS: saturation-absorption spectroscopy, OI: optical isolator, AOM: acousto-optic modulator, PBS: polarization beam splitter.

have a power of 40 μW and a diameter of 3 mm. Two black spots with 3 mm in diameter are placed separately in the centre of the repumping beams, which are combined with depumping beams. By focusing the composite beams, Rb and Cs atoms populate in the lowest states ($F = 2$ for Rb atoms and $F = 3$ for Cs atoms). Atomic clouds are observed by two charge-coupled device (CCD) cameras placed along the horizontal and vertical direction. The atomic density n and atom number N are measured to be $n_{\rm Rb} = 3 \times 10^{11}$ cm^{-3}, $N_{\rm Rb} = 2 \times 10^{8}$, $n_{\rm Cs} = 6 \times 10^{11}$ cm^{-3}, and $N_{\rm Cs} = 3 \times 10^{8}$. Temperatures of the Rb and Cs atomic clouds are measured to be about 100 μk and 70 μk by time-of-flight absorption imaging.

The PA transition is driven by a Ti:sapphire laser with a typical linewidth of less than 100 kHz and output power up to ~600 mW. This beam is focused on the atomic cloud with a Gaussian radius of 500 μm, which can completely cover the ultracold atomic cloud. The frequency of PA is monitored by using a commercial wavelength meter (WS/7R) with an absolute accuracy of 60 MHz. In order to ensure the accuracy of frequency measurement, the wavemeter is calibrated by the Cs atomic hyperfine structure transition.

The ionization laser is a 715-nm pulsed dye laser pumped by a second harmonic of 532-nm Nd:YAG laser at a rate of 10 Hz. The output energy is about 1 mJ with 8 ns duration. Using a lens, the ionization laser is focused on the atomic cloud with a diameter of 1 mm. The typical peak intensity is 2.4×10^{7} W/cm^2. After ionization, the formed ions are accelerated by the electronic field and detected by a micro-channel plate (MCP). These detected ion signals are disposed by a boxcar integrator (SRS-250) and recorded by an NIPCI1714 board. The master clock of the trapping, repumping, PA and ionization laser are controlled by two external delay/pulse generators (SRS, DG 535).

3. Experimental results

We have observed rovibrational serial RbCs* levels corresponding to the $\Omega = (2)0^-$ potential dissociation from the $6P_{1/2}$ limit. Figure 3(a) shows the photoassociation spectrum of RbCs molecules at the $v = 189$ vibrational level, which is obtained by detecting the triplet ground state RbCs molecules. The PA laser is extinguished 100 μs before the ionization pulse so that all the excited molecules have enough time to decay to the triplet states. The frequency of the PA laser is scanned from 11105.9400 cm^{-1} to 11106.0241 cm^{-1} which belongs to a $\Omega = (2)0^-$ vibrational level for RbCs. The selection rules prohibit the path that molecules in the $\Omega = (2)0^-$ excited state decay spontaneously to the $X^1\Sigma^+$ ground state, which has only a $\Omega = 0^+$ component in Hund's case (c) coupling. However, molecules in the $\Omega = (2)0^-$ excited state can decay to the $a^3\Sigma^+$ state, which has $\Omega = 0^-$ and $\Omega = 1^\pm$ components. According to the selection rules and molecular potential curve, we can infer that the observed RbCs$^+$ signal arises from $a^3\Sigma^+ \rightarrow (3)^3\Pi$ transition through RETPI. There is no coupling between angular momentum and nuclear spin for molecules in the $\Omega = (2)0^-$ state. Hence, we can recognize clearly the rotational structure from the spectrum. The molecular ion intensities of different rotational levels are different. One reason is that different rovibrational levels have various PA rates, which is dependent on the Frank–Condon factor (FCF)[19] between the atomic scattering state and the molecular bound state. Another reason is that the spontaneous radiations[20] between the excited state and the ground state molecules are also different for different rotational levels.

According to the nonrigid model,[21] the molecular rovibrational energy can be expressed as

$$\frac{E_v}{hc} = B_v J(J+1) - D_v J^2 (J+1)^2, \ \ J \geq 0, \tag{1}$$

where E_v is the rovibrational energy eigenvalue, h is Planck's constant, c is the speed of light, B_v is the rotational constant of the v vibrational state, D_v is the corresponding centrifugal distortion constant, v is the vibrational quantum number, and J is the rotational quantum number.

The adjacent rotational level interval ΔE reads

$$\Delta E = \frac{E_v(J) - E_v(J-1)}{hc} = 2B_v J - 4D_v J^3, \ \ J \geq 1. \tag{2}$$

Usually, D_v is typically several orders of magnitude smaller than B_v, so we ignore the higher-order term. Thus, formula (2) can be simplified as

$$\Delta E = \frac{E_v(J) - E_v(J-1)}{hc} = 2B_v J, \ \ J \geq 1. \tag{3}$$

Figure 3(b) shows the relationship between the rotational level interval and the rotational quantum number for the molecules we observed. The rotational constant is about 0.00443 cm^{-1} by fitting formula (3). Taking into consideration the fitting error, level interval standard deviation, reference cavity stability error and the nonlinear error of the scan frequency of the PA, the total error of the rotational constant is about 0.00062 cm^{-1}. The $(2)0^-$ state is a weakly bound state, which is bound by several wavenumbers and have outer turning points with a value of about 25 Å. Consequently, the rotational constant $B \approx h^2/8\mu\pi^2R^2$ is small (where μ is the reduced mass, R is the nuclear interval between two atoms).

In 2003, Bergeman *et al.*[22] analyzed the Fourier-transform spectroscopy data from laser-induced fluorescence of the coupled $A^1\Sigma^+$ and $b^3\Pi$ states of RbCs. In addition, they assigned vibrational levels of the $(2)0^-$ state, and calculated the corresponding rotational constants. In 2010, Docenko *et al.*[23] analyzed two sets of experimental Fourier-transform spectroscopy data of the $A^1\Sigma^+$–$b^3\Pi$ complex. One set is from mixed A-b $\rightarrow$ X transition, and the other is from $(4)^1\Sigma^+ \rightarrow$ A-b emission and extends to higher A-b energy levels. From a detailed analysis of the spectroscopy data, they found that the

vibrational number of the A state is raised by one quantum[23] over that reported by Bergerman *et al.*[22] Table 1 shows a comparison between the calculated data and the experimental data of the rotational constant B for some vibrational level positions ($v = 188$–194) of $(2)0^-$ state. The calculated vibrational numbers are modified. In Table 1, the $v = 189$, 190 vibrational levels are observed for the first time. The observations are due to the different detection method compared with Ref. [24]. The dominant interaction term depends on R^{-3} for the homonuclear excited state molecules, while depending on R^{-6} for heteronuclear excited state molecules,[25] where R is the internuclear distance. On the one hand, the photoassociation rate for heteronuclear molecules is lower than that for homonuclear molecules, so it is difficult to measure the photoassociation spectrum of RbCs molecules in some vibrational levels of $(2)0^-$ state by trap loss technique. On the other hand, the spontaneous decay rate to the ground state for heteronuclear molecules is higher than that for homonuclear molecules. For this reason we can use the RETPI to detect ground state RbCs molecules. In addition, the time-of-flight mass spectrum used in our experiment is a highly-sensitive technique to detect the molecules in the ground state. It can even detect a single ion in the optimized conditions.

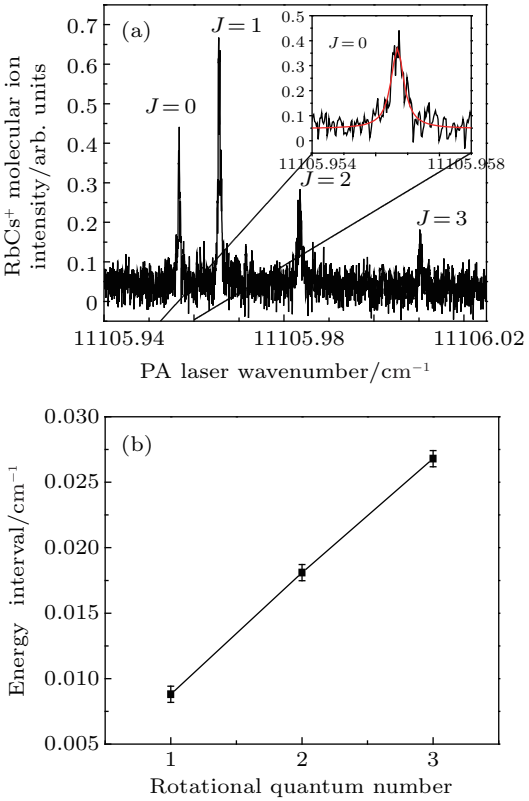


Fig. 3. (color online) (a) Photoassociation spectra of RbCs molecules in the $v = 189$ vibrational level of $(2)0^-$ state. The inset shows the Lorenz fitting to the photoassociation spectrum in the $J = 0$ rotational state. (b) The corresponding rotational constant fitting for the observed vibrational level with formula (3).

Table 1. Comparisons between the calculation results and experimental data of the rotational constants B for some vibrational level positions ($v = 188$–194) of $(2)0^-$ state.

	Calculating data		Experimental data	
v	E/cm^{-1}	B/cm^{-1}	E/cm^{-1}	B/cm^{-1}
188	–78.4131	0.00448	–78.485[b)]	0.00460[b)]
189	–72.5735	0.00436	–72.458[a)]	0.00443[a)]
190	–66.9614	0.00426	–66.703[a)]	0.00422[a)]
191	–61.5177	0.00421	–61.074[b)]	0.00456[b)]
192	–56.3458	0.00404	–55.98[b)]	0.0041[b)]
193	–51.4537	0.00391	–51.099[b)]	0.00389[b)]
194	–46.8061	0.0038	–46.574[b)]	0.00356[b)]

[a)] Experimental measurements of our group; [b)] Ref. [24]. The trap loss technique was used to measure the photoassociation spectrum.

4. Summary

In summary, we cool and trap ^{85}Rb and ^{133}Cs atoms in dual-species, force dark MOT. Then we produce ultracold polar molecules via the PA technique. We detect these molecules in $a^3\Sigma^+$ state using resonance-enhanced two-photon ionization. For scanning PA, we obtain high resolution spectra of RbCs molecules in the $v = 189$ and $v = 190$ vibrational levels of the $(2)0^-$ state, and calculate the corresponding rotational constants (0.00443 and 0.00422 cm^{-1}). We compare the calculated data with experimental data of rotational constants B for some vibrational level positions ($v = 188$–194) of the $(2)0^-$ state. From the study of ultracold polar RbCs molecules, we can have a good knowledge of molecular level structure and the interaction between RbCs molecules and dipolar effects.

Acknowledgment

We thank T Bergeman for helpful discussion and providing us with the calculated data.

References

[1] Ji Z H, Zhang H S, Wu J Z, Yuan J P, Yang Y G, Zhao Y T, Ma J, Wang L R, Xiao L T and Jia S T 2012 *Phys. Rev. A* **85** 013401

[2] Swallows M D, Bishof M, Lin Y, Blatt S, Martin M J, Rey A M and Ye J 2011 *Science* **331** 1043

[3] Rieger T, Junglen T, Rangwala S A, Pinkse P W H and Rempe G 2005 *Phys. Rev. Lett.* **95** 173002

[4] Kuznetsova E, Bragdon T, Côté R and Yelin S F 2012 *Phys. Rev. A* **85** 012328

[5] Thorsten K, Krzysztof G and Julienne P S 2006 *Rev. Mod. Phys.* **78** 1311

[6] Jones K M, Tiesinga E, Lett P D and Julienne P S 2006 *Rev. Mod. Phys.* **78** 483

[7] Li Y Q, Ma J, Wu J Z, Zhang Y C, Zhao Y T, Wang L R, Xiao L T and Jia S T 2012 *Chin. Phys. B* **21** 043404

[8] Ji Z H, Zhang H S, Wu J Z, Yuan J P, Zhao Y T, Ma J, Wang L R, Xiao L T and Jia S T 2011 *Chin. Phys. Lett.* **28** 083701

[9] Wang D, Qi J, Stone M F, Nikolayeva O, Wang H, Hattaway B, Gensemer S D, Gould P L, Eyler E E and Stwalley W C 2004 *Phys. Rev. Lett.* **93** 243005

[10] Haimberger C, Kleinert J, Bhattacharya M and Bigelow N P 2004 *Phys. Rev. A* **70** 021402

[11] Deiglmayr J, Grochola A, Repp M, Mörtlbauer K, Glück C, Lange J, Dulieu O, Wester R and Weidemüller M 2008 *Phys. Rev. Lett.* **101** 133004

[12] Wang H and Stwalley W C 1998 *J. Chem. Phys.* **108** 5767

[13] Pilch K, Lange A D, Prantner A, Kerner G, Ferlaino F, N?gerl H C and Grimm R 2009 *Phys. Rev. A* **79** 042718

[14] Cho H W, McCarron D J, Jenkin D L, Köppinger M P and Cornish S L 2011 *Eur. Phys. J. D* **65** 125

[15] Stwalley W C, Banerjee J, Belos M, Carollo R, Recore M and Mastroianni M 2010 *J. Phys. Chem. A* **114** 81

[16] Londoño B E, Mahecha J E, Luc-Koenig E and Crubellier A 2009 *Phys. Rev. A* **80** 032511

[17] Gabbanini C and Dulieu O 2011 *Phys. Chem. Chem. Phys.* **13** 18905

[18] Wang L R, Ji Z H, Yuan J P, Yang Y, Zhao Y T, Ma J, Xiao L T and Jia S T 2012 *Chin. Phys. B* **21** 113402

[19] Wang C C and Killinger D K 1979 *Phys. Rev. A* **20** 1495

[20] Zhang H S, Ji Z H, Yuan J P, Zhao Y T, Ma J, Wang L R, Xiao L T and Jia S T 2011 *Chin. Phys. B* **20** 123702

[21] Lysebo M and Veseth L 2008 *Phys. Rev. A* **77** 032721

[22] Bergeman T, Fellows C E, Gutterres R F and Amiot C 2003 *Phys. Rev. A* **67** 050501

[23] Docenko O, Tamanis M, Ferber R, Bergeman T, Kotochigova S, Stolyarov A V, Faria N A and Fellows C E 2010 *Phys. Rev. A* **81** 042511

[24] Kerman A J, Sage J M Sainis S, Bergeman T and DeMille D 2004 *Phys. Rev. Lett.* **92** 033004

[25] Ji Z H, Wu J Z, Zhang H S, Meng T F, Ma J, Wang L R, Zhao Y T, Xiao L T and Jia S T 2011 *J. Phys. B* **44** 025202